Canal surfaces as Bézier curves using mass points

Lionel Garnier, Jean-Paul Becar, Lucie Druoton

Canal surfaces as Bézier curves using mass points

Lionel Garnier [a,*], Jean-Paul Bécar [b], Lucie Druoton [c]

[a] LE2i, FRE 2005, CNRS, Arts et Métiers, Univ. Bourgogne Franche-Comté, B.P. 47870, 21 078 Dijon Cedex, France
[b] LAMAV-CGAO, CNRS 2956, Le Mont-Houy, 59313 Valenciennes Cedex 9, France
[c] IMB, UMR CNRS 5584, Univ. Bourgogne Franche-Comté, B.P. 47870, 21 078 Dijon Cedex, France

Abstract :

The paper aims to connect the Bézier curves domain to another known as the Minkowski–Lorentz space for CAGD purposes. The paper details these connections. It provides new algorithms for surface representations and surfaces joining. Some G^1-blends between canal surfaces illustrate the results with a seahorse sketched. It is well known that rational quadratic Bézier curves define conics. Here, the use of mass points offers the definition of a semi-conic or a branch of hyperbola in the Euclidean plane. Moreover, the choice of an adequate non-degenerate indefinite quadratic form makes a non-degenerate central conic seen as a unit circle. That is not possible in the homogeneous coordinates background. The rational quadratic Bézier curves using mass points provide the modelling of canal surfaces with singular points. These are embedded in the Minkowski–Lorentz space. In that space, these curves are circular arcs which look like ellipse or hyperbola arcs. In the Minkowski–Lorentz space, oriented spheres and oriented planes of R^3 are points on the unit sphere, the points of R^3 and the point at infinity are vectors laying on the light-cone. A particular case of canal surfaces is the cyclides of Dupin. In the Minkowski–Lorentz space, the modelling of any Dupin cyclides patch is completed by a family of algorithms. Each family depends only on the number of singularities known for the Dupin cyclide part. The paper ends with an example of a G^1 connection between two Dupin cyclides. All previous results are finally applied in a seahorse shape design.

Keywords:
Mass points
Bézier curves Minkowski–
Lorentz space

1. Introduction

The paper aims to connect the Bézier curves domain to another known as the Minkowski–Lorentz space for CAGD purposes. The paper details these connections. It provides new algorithms for surface representations and surfaces joining. Some G^1-blends between canal surfaces illustrate the results with a sketched seahorse.

In the computer aided domain, the rational Bézier curves play an important role for geometric modelling. The second order curves define a conic arc (Bézier, 1986; De Casteljau, 1985; Garnier, 2007; Bécar, 1997). Such a curve is considered as the set of barycentres of weighted points. However, some problems occur for the representation of non-bounded parabolic or hyperbolic arcs. One answer is the use of weighted points and vectors in the same space (Fiorot and Jeannin, 1989). In that space, any vector is considered as a point with a zero weight. Thus the Bézier curves can be generalized. In the

second order rational curves, by the use of some homographic parameter changes, all features of conics such as focus and directrix can be determined (Bécar, 1997; Garnier and Bécar, 2016). The figures of all the rational quadratic Bézier curves with control mass points are sketched with the *pstricks* package, see https://www.ctan.org/pkg/pst-bezier. The 3D figures are built with an open source software: the Persistence of vision raytracer -POV-Ray- in short (www.povray.org).

Other methods developed by Albrecht (2001), Goldman and Wang (2004), Lee (1985), Sánchez-Reyes (2011) are taking an Euclidean space as background. Here, we give some constructions of elliptical or hyperbolic arcs which are circle arcs for a non-Euclidean metric. Other examples of these models, in the space of spheres, can be found in Garnier et al. (2012, 2015), Garnier and Druoton (2013c). Moreover, some researchers use homogeneous coordinates to model a semi-circle (Versprille, 1975; Piegl and Tiller, 1995; Farin, 1992), but L. Piegl mentions this problem in Piegl and Tiller (1995): *"A point in projective space is what mathematicians call an equivalence class. This means that* $\overrightarrow{P_j}\left(x_j, y_j, z_j, 0\right)$ *and* $\overrightarrow{P_j}^*\left(\alpha x_j, \alpha y_j, \alpha z_j, 0\right)$ *are two representations of the same point in projective space. However, substituting* $\overrightarrow{P_j}$ *and* $\overrightarrow{P_j}^*$ *into Eq. (7.34) clearly results in two different curves."* Using mass points, we choose the vector which allows to obtain a semi-circle, this circle can be Euclidean or not. This vector is defined by using perpendicular conditions and pseudo-metric conditions to determine a Bézier curve which models a given hyperbola seen as a circle (for the non-degenerate indefinite quadratic form), see section 2.2. The reader may consult Albrecht et al. (2008) which gives a modern application of conics in the context of curve approximations and Druoton et al. (2013a), Garnier and Druoton (2013a) where the authors compute the characteristic circles of a Dupin cyclide modelled in the space of spheres.

The background about the space of the oriented spheres and the Minkowski–Lorentz space can be found in Druoton et al. (2014, 2013a, 2013b), Dorst et al. (2007), Garnier and Druoton (2013b), Langevin et al. (2014). Just one of these papers (Druoton et al., 2013b) is a focus on G^1-blends between Dupin cyclides using conics and the aim of this paper is to give conditions to avoid cusps. In Druoton et al. (2013b), a Dupin cyclide is defined by a 2-plane built using a point and two orthogonal vectors for the Lorentz form. Some calculations provide this reference frame. Then, the parametrization of the conic depends on its Euclidean type (ellipse or hyperbola) and the bounds of any arc have to be computed. Then, the tangent vectors must be computed too. The use of Bézier curves permits to have only one parametric set: $[0, 1]$. Moreover, we do not have to compute tangent vector, we do not have to determine the type of the plane containing the conic and an iterative construction of Dupin cyclides blends (see the seahorse) is following. In Foufou and Garnier (2004), using usual rational quadratic Bézier curves, an iterative construction of the principal circle arcs of Dupin cyclides is proposed to illustrate the modelling of Eurographics04 Hugo. In our context, the singular points of Dupin cyclides are vectors. In order to obtain the whole representation of Dupin cyclides, the usual rational quadratic Bézier curves does not match. Thus, the set of the mass points is introduced to fix this problem and the vectors can be bounds of the conic and then, in the 3d Euclidean affine space $\mathcal{E}_3$, singular points are bounds. Moreover, one of these vectors can be $\overrightarrow{e_\infty}$ which represents the point at the infinity of $\mathcal{E}_3$. In fact, there is no difference between the point at the infinity of $\mathcal{E}_3$ and the points of $\mathcal{E}_3$. Then, we can model Dupin cyclides (degenerate or non-degenerate) or pencils of oriented spheres using conics in the Minkowski–Lorentz space and the algorithms depend only on the numbers of the singular points and the representation is the same for: a horned Dupin cyclide, a spindle Dupin cyclide, a spindle torus and a circular cone or a Poncelet pencil of spheres; a circular cylinder, a horn torus, a singly horned Dupin cyclide and a one-singularity spindle Dupin cyclide; a ring torus, a ring Dupin cyclide and a pencil of spheres with a base circle. The connection described offers some applications as a proof and the computation of Dandelin spheres, algorithms for subdivision and iterative construction of joining G^1 canal surfaces.

This paper is organized as follows: the section 2 deals with semi-circles using rational quadratic Bézier curves in the set of the mass points. In Section 3, the Minkowski–Lorentz space is defined. This space contains the space of the oriented spheres and the paraboloid which is isometric with the usual 3D Euclidean affine space. In Section 4, we model a seahorse as an application of modelling with canal surfaces in the usual Euclidean affine space using rational quadratic Bézier curves and mass points in the Minkowski–Lorentz space. Moreover, a G^1 blend of these curves implies a G^1 blend of these canal surfaces (Druoton et al., 2013b; Langevin and Solanes, 2011). The last section draws some conclusion and proposes future works. Appendix A proposes a synthesis about the main results of this paper.

2. Rational quadratic Bézier curves in $\widetilde{\mathcal{P}}$

In the following $\left(O; \vec{\imath}; \vec{\jmath}\right)$ designates a direct reference frame in the usual Euclidean affine plane $\mathcal{P}$ and $\overrightarrow{\mathcal{P}}$ is the set of vectors of the plane. The set of mass points is defined by

$$\widetilde{\mathcal{P}} = \left(\mathcal{P} \times \mathbb{R}^*\right) \cup \left(\overrightarrow{\mathcal{P}} \times \left\{\overrightarrow{0}\right\}\right)$$

On the mass point space, the addition, denoted $\oplus$, is defined as follows:

- $\omega \neq 0 \Longrightarrow (M;\omega) \oplus (N;-\omega) = \left(\omega\ \overrightarrow{NM}; 0\right)$;
- $\omega\,\mu\,(\omega+\mu) \neq 0 \Longrightarrow (M;\omega) \oplus (N;\mu) = \left(\texttt{bar}\left\{(M;\omega);(N;\mu)\right\}; \omega+\mu\right)$ where $\texttt{bar}\left\{(M;\omega);(N;\mu)\right\}$ is the barycentre of the weighted points $(M;\omega)$ and $(N;\mu)$;
- $\left(\vec{u};0\right) \oplus \left(\vec{v};0\right) = \left(\vec{u}+\vec{v};0\right)$;

- $\omega \neq 0 \Longrightarrow (M;\omega) \oplus \left(\overrightarrow{u};0\right) = \left(\mathcal{T}_{\frac{1}{\omega}\overrightarrow{u}}(M);\omega\right)$ where $\mathcal{T}_{\overrightarrow{W}}$ is the translation of $\mathcal{P}$ of vector $\overrightarrow{W}$.

In the same way, on the space $\widetilde{\mathcal{P}}$, we define the multiplication by a scalar, denoted $\odot$, as follows:

- $\omega\alpha \neq 0 \Longrightarrow \alpha \odot (M;\omega) = (M;\alpha\,\omega)$
- $\omega \neq 0 \Longrightarrow 0 \odot (M;\omega) = \left(\overrightarrow{0};0\right)$
- $\alpha \odot \left(\overrightarrow{u};0\right) = \left(\alpha\overrightarrow{u};0\right)$

One can note that $\left(\widetilde{\mathcal{P}},\oplus,\odot\right)$ is a vector space (Garnier and Bécar, 2016). So, a mass point is a weighted point (M,ω) with $\omega \neq 0$ or a vector $\left(\overrightarrow{u},0\right)$. The three quadratic Bernstein polynomials defined by

$$B_0(t) = (1-t)^2\,,\ B_1(t) = 2\,t\,(1-t)\,,\ B_2(t) = t^2\,,\ \ t \in [0,1] \tag{1}$$

provide the definition of rational quadratic Bézier curve (BR curve) in $\widetilde{\mathcal{P}}$ given below.

Definition 1. (Rational quadratic Bézier curve (BR curve) in $\widetilde{\mathcal{P}}$)
Let ω_0, ω_1 and ω_2 be three real numbers.
Let $(P_0;\omega_0)$, $(P_1;\omega_1)$ and $(P_2;\omega_2)$ be three non-collinear mass points in $\widetilde{\mathcal{P}}$.
Define two sets

$$I = \{i \mid \omega_i \neq 0\} \ \text{ and } \ J = \{i \mid \omega_i = 0\}$$

Define the function ω_f as follows

$$\begin{array}{rccl} \omega_f : & [0;1] & \longrightarrow & \mathbb{R} \\ & t & \longmapsto & \omega_f(t) = \displaystyle\sum_{i\in I} \omega_i \times B_i(t) \end{array} \tag{2}$$

A mass point $(M;\omega)$ or $\left(\overrightarrow{u};0\right)$ belongs to the quadratic Bézier curve defined by the three control mass points $(P_0;\omega_0)$, $(P_1;\omega_1)$ and $(P_2;\omega_2)$, if there is a real t_0 in $[0;1]$ such that:

- if $\omega_f(t_0) \neq 0$ then

$$\begin{cases} \overrightarrow{OM} = \dfrac{1}{\omega_f(t_0)}\left(\displaystyle\sum_{i\in I} \omega_i\, B_i(t_0)\ \overrightarrow{OP_i}\right) + \dfrac{1}{\omega_f(t_0)}\left(\displaystyle\sum_{i\in J} B_i(t_0)\ \overrightarrow{P_i}\right) \\ \\ \omega = \omega_f(t_0) \end{cases} \tag{3}$$

- if $\omega_f(t_0) = 0$ then

$$\overrightarrow{u} = \sum_{i\in I} \omega_i B_i(t_0)\,\overrightarrow{OP_i} + \sum_{i\in J} B_i(t_0)\,\overrightarrow{P_i} \tag{4}$$

Such a curve is denoted $BR\{(P_0;\omega_0);(P_1;\omega_1);(P_2;\omega_2)\}$. □

If $J = \emptyset$, this definition leads to the usual rational quadratic Bézier curve.
This kind of curve can model a circular arc as detailed in the next result.

2.1. Modelling Euclidean circular arcs

Theorem 1. *Let C be a circle of centre O_0 and of radius R.*
Let P_0 and P_2 be two points belonging to the circle C.
Let ω_0 and ω_2 be two positive reals.

- *If O_0 is not the midpoint of the segment $[P_0P_2]$*
  Let I_1 be the midpoint of the segment $[P_0P_2]$.
  Define the point P_1 as

$$\overrightarrow{I_1P_1} = t_1\overrightarrow{O_0I_1} \ \ \textit{with} \ \ t_1 = \frac{\overrightarrow{O_0P_0}\bullet\overrightarrow{I_1P_0}}{\overrightarrow{O_0P_0}\bullet\overrightarrow{O_0I_1}} \tag{5}$$

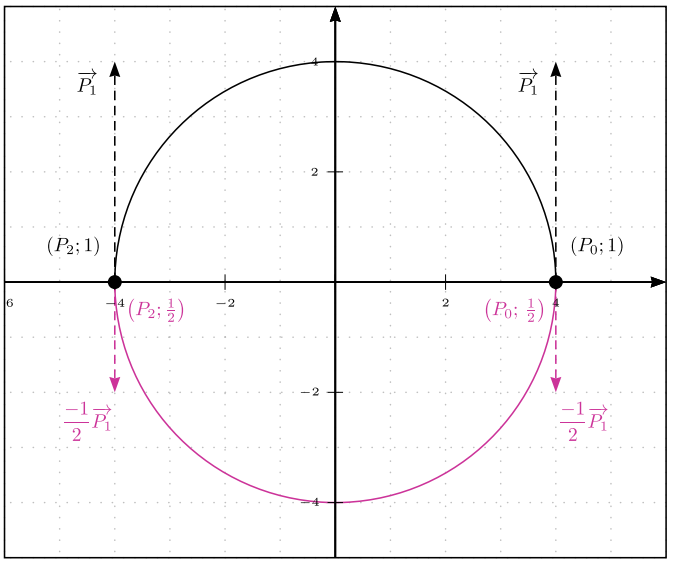

Fig. 1. Two semi-circles defined as BR curves using the second part of Theorem 1. The Bézier curves are drawn using *pstricks* package.

The BR $\{(P_0;\omega_0);(P_1;\omega_1);(P_2;\omega_2)\}$ *is a circular arc iff*

$$\omega_1^2 = \omega_0\,\omega_2\,\cos^2\left(\widehat{\overrightarrow{P_0P_1};\overrightarrow{P_0P_2}}\right) \tag{6}$$

- *If* O_0 *is the midpoint of the segment* $[P_0P_2]$
  The BR $\left\{(P_0;\omega_0);\left(\left(\overrightarrow{P_1};0\right)\right);(P_2;\omega_2)\right\}$ *is a semi-circle of C iff*

$$\begin{cases} \overrightarrow{P_1}\bullet\overrightarrow{P_0P_2} &= 0 \\ \omega_0\,\omega_2\,\overrightarrow{P_0P_2}^2 &= 4\,\overrightarrow{P_1}^2 \end{cases} \tag{7}$$

Proof. See Garnier (2007) for Formulae (5) and (6) and Proposition 5.4.2 of Fiorot and Jeannin (1989). □

To obtain the black curve in Fig. 1, the control mass points of the black curve are $(P_0;1)$, $\left(\overrightarrow{P_1};0\right)$, and $(P_2;1)$ i.e. the weights ω_0 and ω_2 are equal to one and it is always possible to obtain this case after a parameter change (Garnier and Bécar, 2016). The control mass points of the magenta curve are $\left(P_0;\frac{1}{2}\right)$, $\left(-\frac{1}{2}\overrightarrow{P_1};0\right)$, and $\left(P_2;\frac{1}{2}\right)$.

2.2. Circles, pseudo-circles and central conics

In an orthogonal frame, the hyperbola of equation $\frac{x^2}{a^2}-\frac{y^2}{b^2}=1$ can be seen as a unit circle taking account of the quadratic form $\mathcal{Q}_{\mathrm{H}}\left(\overrightarrow{u}\right)=\frac{x^2}{a^2}-\frac{y^2}{b^2}$ where $\overrightarrow{u}\ (x,y)$. The BR representation of the hyperbola can be chosen similar to the representation seen in Theorem 1. Theorem 2 focuses on that point.

Theorem 2. *Let* $H = BR\{(P_0;1),(P_1;\omega_1),(P_2;1)\}$ *with* $\omega_1 > 1$.
Define $\varepsilon\in\{-1;1\}$.
The homographic parameter change,

$$\begin{aligned} h:\ \overline{\mathbb{R}} &\longrightarrow \overline{\mathbb{R}} \\ u &\longmapsto \frac{\dfrac{\varepsilon}{\sqrt{\omega_1^2-1}}u}{1-u+\varepsilon\dfrac{1-\omega_1}{\sqrt{\omega_1^2-1}}u} \end{aligned} \tag{8}$$

provides the new representation of $H = BR\left\{(Q_0;1);\left(\overrightarrow{Q_1};0\right);(Q_2;-1)\right\}$ *where*

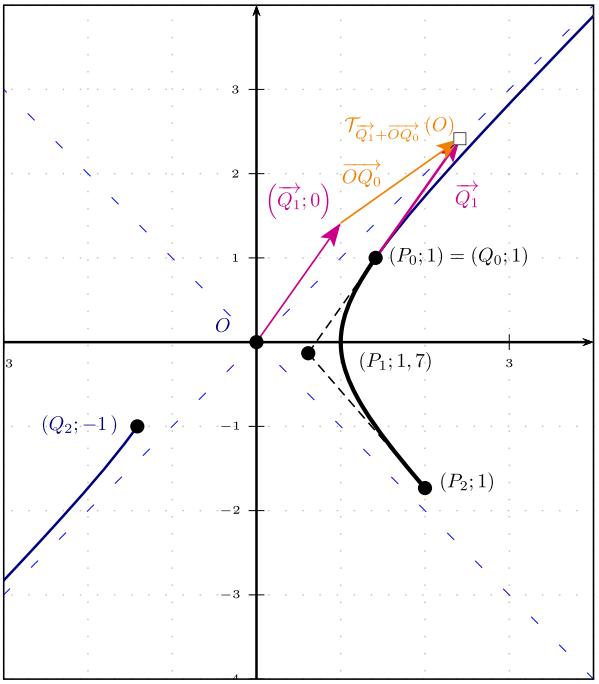

Fig. 2. A hyperbola seen as a circle of centre O. The curve $BR\{(Q_0;1);\left(\overrightarrow{Q_1};0\right);(Q_2;-1)\}$, obtained from the curve $BR\{(P_0;1);(P_1;\omega_1);(P_2;1)\}$, is a semi-circle. The point $\mathcal{T}_{\overrightarrow{Q_1}+\overrightarrow{OQ_0}}(O)$, image of the point O by the translation of vector $\overrightarrow{Q_1}+\overrightarrow{OQ_0}$, belongs to one of the two asymptotes of the circle.

$$\begin{cases} (Q_0;1) &= (P_0;1) \\ \left(\overrightarrow{Q_1};0\right) &= \left(\dfrac{\varepsilon\,\omega_1}{\sqrt{\omega_1^2-1}}\overrightarrow{P_0P_1};0\right) \\ (Q_2;-1) &= \mathtt{bar}\left\{\left(P_0;\dfrac{\omega_1^2}{\omega_1^2-1}\right);\left(P_1;\dfrac{-2\,\omega_1^2}{\omega_1^2-1}\right);\left(P_2;\dfrac{1}{\omega_1^2-1}\right)\right\} \end{cases}$$

Proof. By the use of Theorem 1 of Garnier and Bécar (2016). □

In Fig. 2, the BR curve of control mass points $(Q_0;1)$, $\left(\overrightarrow{Q_1};0\right)$ and $(Q_2;-1)$ is a semi-circle of the unit circle H. Moreover

$$\lim_{t\to\frac{1}{2}}(Q_0;B_0(t))\oplus\left(B_1(t)\ \overrightarrow{Q_1};0\right)\oplus(Q_2;-B_2(t))=\left(\frac{1}{2}\left(\overrightarrow{OQ_0}+\overrightarrow{Q_1}\right);0\right)$$

The reader can note that Formula (7) is still true given that

$$1\times-1\times\mathcal{Q}_{\mathrm{H}}\left(\overrightarrow{Q_0Q_2}\right)=-4=4\times\mathcal{Q}_{\mathrm{H}}\left(\overrightarrow{Q_1}\right)$$

but the result is negative, the point Q_1 defined by $\overrightarrow{OQ_1}=\overrightarrow{Q_1}$ does not belong to the circle H.
Moreover, the position tangent vectors to the curve $BR\{(Q_0;1);\left(\overrightarrow{Q_1};0\right);(Q_2;-1)\}$ which define the unit circle H of centre O generate a dual circle H* of centre O and the square of its radius is -1.

The last representation can be considered as a semi-circle of H when the parameter runs in $[0;1]$, see Fig. 2. These results are setting the basics of the Minkowski–Lorentz space in order to work with spheres, canal surfaces and Dupin cyclides.

3. The Minkowski–Lorentz space and the space of spheres Λ^4

The Minkowski–Lorentz space $\overrightarrow{L_{4,1}}$ is the real vector space of dimension 5. The symmetric bilinear form $\mathcal{L}_{4,1}$ denoted by a dot product, is defined on the canonical basis $(\overrightarrow{e_-},\overrightarrow{e_1},\overrightarrow{e_2},\overrightarrow{e_3},\overrightarrow{e_+})$ as follows

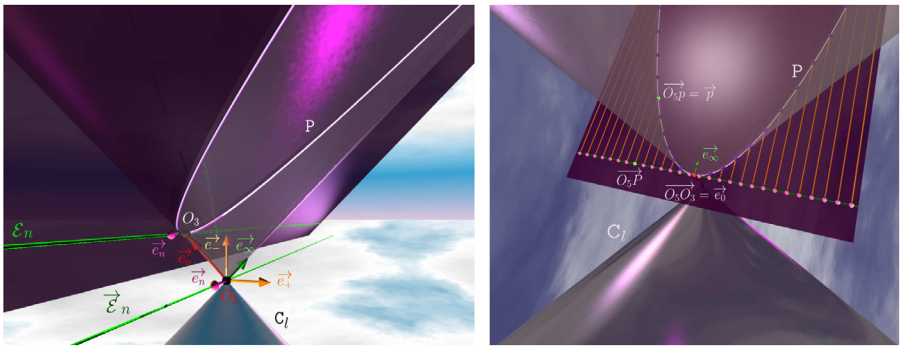

(a) (b)

Fig. 3. Construction of the 3-dimensional paraboloid P isometric to the usual 3-dimensional Euclidean affine space $\mathcal{E}_3$. The type of $\vec{e_\infty}$, $\vec{e_o}$, $\vec{\mathcal{H}}$. The hyperplane $\vec{\mathcal{H}}$ is tangent to C_l. Each light-like vector $\vec{n_2}$, such as $\vec{n_2}$ and $\vec{e_\infty}$ are not collinear, defines a point of $\mathcal{E}_3$ via the paraboloid P: the point is the intersection between the line $(O; \vec{n_2})$ and the paraboloid P.

$$\vec{e_i} \cdot \vec{e_j} = 0 \text{ if } i \neq j,\ \vec{e_-} \cdot \vec{e_-} = -1 \text{ and } \vec{e_i} \cdot \vec{e_i} = 1 \tag{9}$$

with $i \in \{1, 2, 3, +\}$ and $j \in \{-, 1, 2, 3, +\}$.

Let $\mathcal{Q}_{4,1}$ be the quadratic form associated to $\mathcal{L}_{4,1}$. The affine Minkowski–Lorentz space $L_{4,1}$ is defined by the point $O_5 = (0, 0, 0, 0, 0)$ and $\overrightarrow{L_{4,1}}$.
A new basis $(\vec{e_o}, \vec{e_1}, \vec{e_2}, \vec{e_3}, \vec{e_\infty})$ with $\vec{e_o} = \vec{e_-} - \vec{e_+}$ and $\vec{e_\infty} = \frac{1}{2}(\vec{e_-} + \vec{e_+})$ eases to embed the usual 3D Euclidean affine space $\mathcal{E}_3$ in the Minkowski–Lorentz space. The reader will check that $\vec{e_o} \cdot \vec{e_o} = \vec{e_\infty} \cdot \vec{e_\infty} = 0$ and $\vec{e_o} \cdot \vec{e_\infty} = -1$.

The origin point O_3 of $\mathcal{E}_3$ is obtained by $\vec{e_o} = \overrightarrow{O_5O_3}$ and the vector $\vec{e_\infty}$ represents the point at infinity of $\mathcal{E}_3$.

According to Minkowski definitions, any vector $\vec{u} \in \overrightarrow{L_{4,1}}$ such that $\mathcal{Q}_{4,1}(\vec{u})$ is negative, positive or zero is qualified as a time-like, space-like or light-like vector respectively. In $L_{4,1}$, the light cone C_l is defined by

$$C_l = \left\{ M \in L_{4,1} \mid \mathcal{Q}_{4,1}\left(\overrightarrow{O_5M}\right) = \overrightarrow{O_5M}^2 = 0 \right\} \tag{10}$$

Let P be a point in $\mathcal{E}_3$ and $\vec{P} = \overrightarrow{O_3P}$ its position vector. Then, the representation of the point P is the point p or the position vector $\vec{p}$ given by

$$\overrightarrow{O_5p} = \vec{p} = \vec{e_o} + \vec{P} + \frac{1}{2}\left\|\vec{P}\right\|^2 \vec{e_\infty}. \tag{11}$$

It can be noticed that the point P defined by

$$\overrightarrow{O_5P} = \overrightarrow{O_5O_3} + \overrightarrow{O_3P} = \vec{e_o} + \vec{P}$$

belongs to the embedding of $\mathcal{E}_3$ in $L_{4,1}$. After some calculations, it yields $\vec{p} \cdot \vec{p} = 0$ thus the point p representing the point P in $\mathcal{E}_3$ lays on the light cone C_l. In fact, the set of these points p defines a 3-dimensional paraboloid P on the hyperplane defines by the point O_3 and the vectors $\vec{e_1}$, $\vec{e_2}$, $\vec{e_3}$, $\vec{e_\infty}$. The axis of P is the line defined by O_3 and the light-like vector $\vec{e_\infty}$ and then, the paraboloid P is isometric to $\mathcal{E}_3$. Conversely, the light-like vector $\vec{p}$ $(x_0; x; y; z; x_\infty)$ represents the point $P\left(\frac{x}{x_0}; \frac{y}{x_0}; \frac{z}{x_0}\right)$ of $\mathcal{E}_3$ if $x_0 \neq 0$ or the point at infinity of $\mathcal{E}_3$ in the direction of $\vec{e_\infty}$ if $x_0 = 0$, see in Fig. 3.

In the rest of this paper, M designates a point of $\mathcal{E}_3$. Its representation in the Minkowski–Lorentz space is noted m or $\vec{m}$ through misuse of language.

3.1. The space of spheres Λ^4

In the Euclidean affine space $\mathcal{E}_3$, each sphere S, of centre Ω, with a non-negative radius r, defines two oriented spheres S^+ and S^-. The inside space and the outside space of S can be distinguished as follows. If the interior (resp. exterior) of the sphere is bounded (resp. non-bounded), the radius of the oriented sphere S^+ (resp. S^-) is $\rho = r$ (resp. $\rho = -r$). The sphere S^+ (resp. S^+) is such that the unit normal vector $\vec{N}$ at the point M is in the same direction (resp. opposite direction) as the vector $\overrightarrow{\Omega M}$. It yields for both cases

$$\overrightarrow{\Omega M} = \rho \vec{N} \tag{12}$$

with $|\rho| = r$.

In the Minkowski–Lorentz space, the representation of the oriented sphere with centre Ω and algebraic radius ρ in $\mathcal{E}_3$ is given by Dorst et al. (2007):

$$\overrightarrow{\sigma} = \frac{1}{\rho}\left(\overrightarrow{e_o} + \overrightarrow{O_3\Omega} + \frac{1}{2}\left(\left\|\overrightarrow{O_3\Omega}\right\|^2 - \rho^2\right)\overrightarrow{e_\infty}\right). \tag{13}$$

In the same way, the oriented plane $\mathcal{P}$ is defined by the point P and the unit normal vector $\overrightarrow{N}$ by

$$\overrightarrow{\pi} = \overrightarrow{N} + \left(\overrightarrow{N} \cdot \overrightarrow{O_3P}\right)\overrightarrow{e_\infty} = \overrightarrow{N} + \left(\overrightarrow{N} \cdot \overrightarrow{P}\right)\overrightarrow{e_\infty}$$

and $\overrightarrow{\pi}^2 = \overrightarrow{N}^2 = 1$. Thus, the unit sphere[1] of $L_{4,1}$

$$\Lambda^4 = \left\{\sigma \in L_{4,1} \mid \overrightarrow{O_5\sigma}^2 = 1\right\} \tag{14}$$

is called the space of spheres, representing the oriented spheres and the oriented planes of $\mathcal{E}_3$. Planes can be considered as spheres passing through the point at infinity of $\mathcal{E}_3$.

Working in the Minkowski–Lorentz space leads some calculations in a linear form rather quadratic combination in $\mathcal{E}_3$ as detailed in Theorems 3 and 4.

3.2. Decrease of the degree calculations

The first theorem gives, in the Minkowski–Lorentz space, the condition to determine if a point belongs to a sphere or not.

Theorem 3. *(Relative position of a point and a sphere or a plane)*
In $\mathcal{E}_3$, let $\mathcal{S}$ be a sphere of centre Ω and of radius ρ. Let $\overrightarrow{\sigma}$ be the representation of $\mathcal{S}$ on Λ^4.
In $\mathcal{E}_3$, let $\mathcal{P}$ be a plane passing through the point P_0, $\overrightarrow{N}$ one of the two unit normal vector.
Let $\overrightarrow{\pi}$ be the representation of $\mathcal{P}$ on Λ^4.
Let P be a point in $\mathcal{E}_3$ and $\overrightarrow{p}$ its representation using the paraboloid $\mathtt{P}$, then:

i/
$$\overrightarrow{\sigma} \cdot \overrightarrow{p} = -\frac{\chi_{\mathcal{S}}(P)}{2\rho} = -\frac{1}{2\rho}\left(\Omega P^2 - \rho^2\right) = 0 \Longleftrightarrow P \in \mathcal{S} \tag{15}$$

ii/
$$\overrightarrow{\pi} \cdot \overrightarrow{p} = \overrightarrow{N} \bullet \overrightarrow{P_0P} = 0 \Longleftrightarrow P \in \mathcal{P} \tag{16}$$

Proof. Bécar et al. (2016), Garnier and Bécar (2017). □

The Euclidean distance between the point P and the plane $\mathcal{P}$ in $\mathcal{E}_3$ is equal to the number $\left|\overrightarrow{\pi} \cdot \overrightarrow{p}\right|$.

The motivation of the choice of light-like vectors (via the paraboloid $\mathtt{P}$) to model the points of $\mathcal{E}_3$ rather than the embedding of $\mathcal{E}_3$ in the Minkowski–Lorentz space is due to the fact that quadratic computations are simplified into linear calculus in $\overrightarrow{L_{4,1}}$ (refer to Formula (15) for example). Moreover, the point p defined by $\overrightarrow{O_5p} = \overrightarrow{p}$ belongs to $\mathtt{P} \cap \mathcal{H}_{\sigma^\perp}$ where $\mathcal{H}_{\sigma^\perp}$ is the hyperplane passing through O_5 with $\overrightarrow{\sigma}$ as gradient: the intersection between $\mathtt{P}$ and $\mathcal{H}_{\sigma^\perp}$ is the set of points of the sphere (in $\mathcal{E}_3$) represented by σ. In the rest of this paper, a plane is a sphere with an infinite radius. The second theorem provides the conditions for the relative positions of two spheres.

Theorem 4. *(Relative positions of two spheres)*
Let $\mathcal{S}$ and $\mathcal{S}_x$ be two oriented spheres in $\mathcal{E}_3$. Let σ and σ_x be their representations on Λ^4. Then, three cases arise:

- *$\mathcal{S} \cap \mathcal{S}_x$ is a circle if and only if $\left|\overrightarrow{O_5\sigma} \cdot \overrightarrow{O_5\sigma_x}\right| < 1$. Moreover, $\mathcal{S}$ and $\mathcal{S}_x$ are orthogonal iff*

$$\overrightarrow{O_5\sigma} \cdot \overrightarrow{O_5\sigma_x} = 0 \tag{17}$$

- *$\mathcal{S}$ and $\mathcal{S}_x$ are tangent if and only if $\left|\overrightarrow{O_5\sigma} \cdot \overrightarrow{O_5\sigma_x}\right| = 1$*
- *$\mathcal{S} \cap \mathcal{S}_x = \emptyset$ if and only if $\left|\overrightarrow{O_5\sigma} \cdot \overrightarrow{O_5\sigma_x}\right| > 1$*

Proof. Garnier and Druoton (2013b), Druoton (2013), Dorst et al. (2007), Garnier and Bécar (2017). □

[1] Seen as a 4-dimensional one-sheeted hyperboloid.

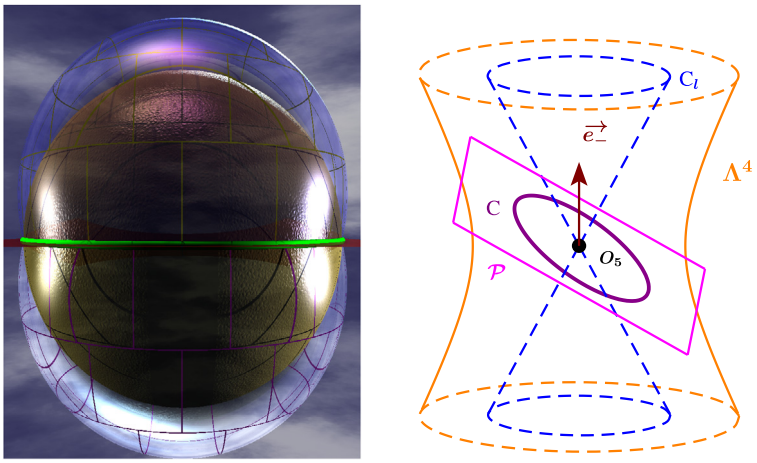

(a) (b)

Fig. 4. A pencil of spheres with a base circle. (a): In $\mathcal{E}_3$. (b): A unit circle of centre O_5, section of Λ^4 by a space-like 2-plane.

3.3. One-parameter family of oriented spheres

A one parameter family of oriented spheres is a curve on Λ^4. The derivative spheres can be defined as follows.

Definition 2. (Derivative sphere)
Let γ be a $\mathcal{C}^1$ curve, defined on the interval I, on Λ^4. The parameterisation of the curve satisfies the following conditions:

- the curve is at least $\mathcal{C}^1$;
- the tangent vectors to the curve are always space-like vectors.

The intersection between Λ^4 and the line defined by O_5 and $\overrightarrow{\frac{\partial \gamma}{\partial \theta}}(\theta_0)$ is a sphere $\dot{\gamma}(\theta_0)$ which is orthogonal to the sphere $\gamma(\theta_0)$ e.g.

$$\overrightarrow{O_5\,\dot{\gamma}(\theta_0)} \cdot \overrightarrow{O_5\gamma(\theta_0)} = 0 \tag{18}$$

□

Moreover, if $\dot{\gamma}(\theta_0)$ (resp. $\gamma(\theta_0)$) represents the sphere $\dot{\mathbb{S}}$ (resp. $\mathbb{S}$), then $\dot{\mathbb{S}} \cap \mathbb{S}$ is a circle, called characteristic circle if γ models a canal surface. The canal Surface and the sphere $\gamma(\theta_0)$ are tangent along the circle $\dot{\mathbb{S}} \cap \mathbb{S}$. So to obtain a G^1 blend between two canal surfaces, it is sufficient that, on Λ^4, the two curves have parallel tangent vectors at the common point (Druoton et al., 2013b). The use of Bézier curves is very interesting for this type of blends.

In Langevin and Walczak (2008), the authors recall that any linear pencil of spheres of $\mathcal{E}_3$ with a base circle is represented in $L_{4,1}$ by the section of the quadric Λ^4 by an affine space-like 2-plane $\mathcal{P}$ passing through O_5, see Fig. 4.

If C is a great circle on the oriented sphere $\mathbb{S}$, and if $\mathcal{P}$ is an oriented plane containing the circle C, then, an expression (on Λ^4) of a sphere which belongs to the pencil of spheres with C as base circle is given by

$$\overrightarrow{O_5\gamma_\theta(\theta)} = \cos(\theta)\ \overrightarrow{O_5\sigma_{\theta_I}} + \sin(\theta)\ \overrightarrow{O_5\sigma^\perp_{\theta_I}} \tag{19}$$

where $\theta \in [0, 2\pi]$ and σ_{θ_I} (respectively $\sigma^\perp_{\theta_I}$) is the representation of the oriented sphere $\mathbb{S}$ (respectively the oriented plane $\mathcal{P}$). Moreover

$$\overrightarrow{O_5\sigma_{\theta_I}} \cdot \overrightarrow{O_5\sigma^\perp_{\theta_I}} = 0$$

From Formula (19), the derivative sphere $\dot{\gamma}_\theta(\theta)$ of the sphere $\gamma_\theta(\theta)$ satisfies

$$\overrightarrow{O_5\,\dot{\gamma}_\theta(\theta)} = -\sin(\theta)\ \overrightarrow{O_5\sigma_{\theta_I}} + \cos(\theta)\ \overrightarrow{O_5\sigma^\perp_{\theta_I}} \tag{20}$$

Conics on Λ^4 represent pencils of spheres or Dupin cyclide. A Dupin cyclide is a canal surface in two ways. So, the representation of a Dupin cyclide on Λ^4 is the union of two conics, one is a connected circle, the other is a circle (connected

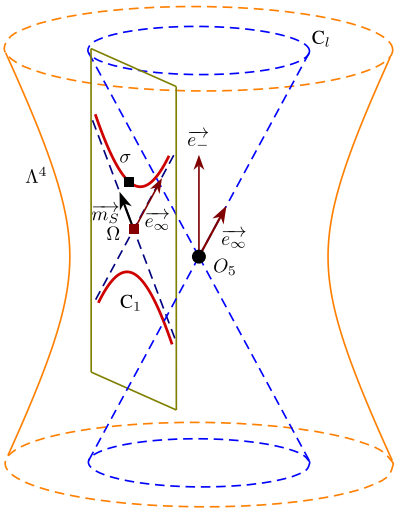

Fig. 5. A circular cone defined by a circle using a rational quadratic Bézier curve. The curve is defined by the point σ and the light-like vectors $\overrightarrow{e_\infty}$ and $\overrightarrow{m_S}$. Let Ω be the centre of the circle. The control mass points of the Bézier curves are $(\overrightarrow{e_\infty}; 0)$, $(\Omega; \omega_1)$ and $(\overrightarrow{m_S}; 0)$ on one hand and $(\overrightarrow{e_\infty}; 0)$, $(\Omega; -\omega_1)$ and $(\overrightarrow{m_S}; 0)$ one the other hand.

or with two branches) or an affine parabola isometric to a line (Druoton et al., 2013a, 2013b, 2014; Garnier and Druoton, 2013b). So, it is usual to model conic arcs by rational quadratic Bézier curves, but, if the Dupin cyclide has one or two singular point(s), the conic leaves the space of spheres Λ^4 and passes through the light-cone via one or two light-like vector(s). Mass points, section 2, are used in the next section to model curves using both points and vectors.

4. Bézier curves and conics in the Minkowski–Lorentz space

In this section, a seahorse using conic arcs in the Minkowski–Lorentz space is built. These conic arcs are computed using rational quadratic Bézier curves. First, the algorithms compute the control points and the weights. The seahorse is next completed.

4.1. Computation of rational quadratic Bézier curves

In this section, the first and last control points can be a point on Λ^4 (e.g. an oriented sphere in $\mathcal{E}_3$) or a light-like vector (e.g. a point in $\mathcal{E}_3 \cup \{\infty\}$).

4.1.1. Cone of revolution defined by its vertex and a sphere

In $\mathcal{E}_3$, a circular cone is defined by spheres and two points: its vertex S and the point at infinity which belongs to every circular cone. These points, in the Minkowski–Lorentz space, are represented by two light-like vectors $\overrightarrow{m_S}$ and $\overrightarrow{e_\infty}$. To define a cone of revolution, it is sufficient to add a sphere $\mathbb{S}$ represented by σ on Λ^4, see Fig. 5. The Bézier curve is a branch of a circle[2] and the light-like vectors $\overrightarrow{m_S}$ and $\overrightarrow{e_\infty}$ and the centre of this circle define the asymptotes to this curve.

The first and last control points are $(\overrightarrow{m_S}; 0)$ and $(\overrightarrow{e_\infty}; 0)$. The intermediate point (Ω, ω_1) is computed using Algorithm 1 as follows. In Minkowski–Lorentz space, the centre Ω of the circle is defined by

$$\overrightarrow{\sigma\Omega} = \alpha\,\overrightarrow{m_S} + \beta\,\overrightarrow{e_\infty} \tag{21}$$

The point Ω is the orthogonal projection of O_5 into the 2-plane $\mathcal{P}_1$ defined by σ, $\overrightarrow{m_S}$ and $\overrightarrow{e_\infty}$. The real numbers α and β are thus computed from the following system

$$\begin{cases} \overrightarrow{O_5\Omega} \cdot \overrightarrow{m_S} = 0 \\ \overrightarrow{O_5\Omega} \cdot \overrightarrow{e_\infty} = 0 \end{cases} \tag{22}$$

Formula (21) implies

$$\overrightarrow{O_5\Omega} = \overrightarrow{O_5\sigma} + \alpha\,\overrightarrow{m_S} + \beta\,\overrightarrow{e_\infty}$$

and the System (22) is equivalent to the system

[2] From an Euclidean point of view, the curve is seen as a branch of a hyperbola.

$$\begin{cases} \overrightarrow{O_5\sigma} \cdot \overrightarrow{m_S} + \beta\, \overrightarrow{e_\infty} \cdot \overrightarrow{m_S} = 0 \\ \overrightarrow{O_5\sigma} \cdot \overrightarrow{e_\infty} + \alpha\, \overrightarrow{m_S} \cdot \overrightarrow{e_\infty} = 0 \end{cases}$$

The solution $(\alpha; \beta)$ of this system leads to Formula (27).

Then, a point $\gamma(t)$ on the Bézier curve verifies

$$\overrightarrow{O_5\gamma(t)} = \overrightarrow{O_5\Omega} + \frac{1}{\omega_1 B_1(t)} \left(B_0(t)\, \overrightarrow{m_S} + B_2(t)\, \overrightarrow{e_\infty} \right) \tag{23}$$

and the last step is the computation of the weight ω_1. To compute ω_1, $t = \frac{1}{2}$ implies

$$\overrightarrow{O_5\gamma\left(\frac{1}{2}\right)} = \frac{2}{\omega_1} \left(\frac{1}{4} \overrightarrow{m_S} + \frac{1}{2} \omega_1 \overrightarrow{O_5\Omega} + \frac{1}{4} \overrightarrow{e_\infty} \right) \tag{24}$$

The point $\gamma\left(\frac{1}{2}\right)$ belongs to Λ^4 iff

$$4\omega_1^2 = \left(\overrightarrow{m_S} + 2\omega_1 \overrightarrow{O_5\Omega} + \overrightarrow{e_\infty} \right)^2 \tag{25}$$

which is equivalent to

$$4\omega_1^2 = 4\omega_1^2 \overrightarrow{O_5\Omega}^2 + 2\overrightarrow{m_S} \cdot \overrightarrow{e_\infty} \tag{26}$$

Computing in the space of spheres eases the calculations due to simplifications, Formula (26) is obtained from Formula (25) since

$$\overrightarrow{m_S}^2 = \overrightarrow{e_\infty}^2 = \overrightarrow{m_S} \cdot \overrightarrow{O_5\Omega} = \overrightarrow{e_\infty} \cdot \overrightarrow{O_5\Omega} = 0$$

So ω_1 is solution of the Equation (28) and each solution ω_1 leads to a circular cone of vertex S.

Algorithm 1 Construction of a circular cone from a point and a sphere.

Input: A point S and a sphere $\mathbb{S}$ where $\chi_{\mathbb{S}}(S) > 0$

1. Compute the light-like vector $\overrightarrow{m_S}$ defined by the vertex S
2. Compute the point σ on Λ^4, defined by the sphere $\mathbb{S}$
3. Compute the centre Ω of the circle by

$$\overrightarrow{O_5\Omega} = \overrightarrow{O_5\sigma} - \frac{\overrightarrow{O_5\sigma} \cdot \overrightarrow{e_\infty}}{\overrightarrow{m_S} \cdot \overrightarrow{e_\infty}} \overrightarrow{m_S} - \frac{\overrightarrow{O_5\sigma} \cdot \overrightarrow{m_S}}{\overrightarrow{m_S} \cdot \overrightarrow{e_\infty}} \overrightarrow{e_\infty} \tag{27}$$

4. Compute the weight ω_1, using the following formula

$$\omega_1^2 = \frac{1}{2} \frac{\overrightarrow{m_S} \cdot \overrightarrow{e_\infty}}{1 - \overrightarrow{O_5\Omega}^2} \tag{28}$$

Output: On Λ^4, a rational quadratic Bézier curve with control mass points $(\overrightarrow{m_S}; 0)$, $(\Omega; \omega_1)$ and $(\overrightarrow{e_\infty}; 0)$.

The algorithms in this section do not distinguish between non-degenerate Dupin cyclide (Dutta et al., 1993), circular cylinder, circular cone or torus. They are only based on the number of singular points on the useful part of the surface. If the vector $\overrightarrow{e_\infty}$ is replaced by a light-like vector $\overrightarrow{m_\infty}$, Algorithm 1 provides a spindle or horned Dupin cyclide. Like the union of the paraboloid with $\overrightarrow{e_\infty}$ is an Alexandroff compactification of $\mathcal{E}_3$, it is possible to send the point represented by $\overrightarrow{m_\infty}$ to the point at infinity of $\mathcal{E}_3$ represented by $\overrightarrow{e_\infty}$ and the Dupin cyclide becomes a cone.

4.1.2. Canal surface defined by a characteristic circle and a point

In this section, a Dupin cyclide is computed under three constraints:

1. a point M_0 which defines the light-like vector $\overrightarrow{m_0}$;
2. a sphere and its derivative one defining a characteristic circle C_0 on the pencil of spheres.

The centre (resp. radius) of the circle is O_0 (resp. r_0). The pencil is defined by the sphere of centre O_0 and of radius r_0 and the plane $\mathcal{P}_0$ containing the circle C_0. Let σ_0 (resp. π_0) be the representation of $\mathbb{S}_0$ (resp. $\mathcal{P}_0$) on Λ^4. The equation of the pencil is given by Formula (19). Next, the value t_1 is chosen to start with two orthogonal spheres of this pencil:

Algorithm 2 A Dupin cyclide patch defined by a point and two orthogonal spheres.

Input: In $\mathcal{E}_3$, a point M_0 and two orthogonal spheres $\mathtt{S}_1$ and $\dot{\mathtt{S}}_1$.

1. Compute the light-like vector $\overrightarrow{m_0}$ which represents the point M_0 via the paraboloid $\mathtt{P}$
2. Compute the point σ_1 on Λ^4 which represents the sphere $\mathtt{S}_1$
3. Compute the point $\dot{\sigma}_1$, on Λ^4 which represents the sphere $\dot{\mathtt{S}}_1$
4. Compute of the centre Ω of the circle in the plane $\mathcal{P}_1$ using Formula (31).
5. Compute of the point P_1 by

$$\overrightarrow{\Omega P_1} = \frac{\overrightarrow{\Omega\sigma_1}^2}{\overrightarrow{m_0} \cdot \overrightarrow{\Omega\sigma_1}} \overrightarrow{m_0} \tag{29}$$

6. Compute of the weight ω_1, solution of the following equation

$$\omega_1^2 = -\frac{\overrightarrow{O_5\sigma_1} \cdot \overrightarrow{m_0}}{2\,\overrightarrow{\sigma_1 P_1}^2} \tag{30}$$

Output: On Λ^4, a rational quadratic Bézier curve $\gamma_{\mathtt{S}}$ with control mass points $(\sigma_1; 1)$, $(P_1; \omega_1)$ and $(\overrightarrow{m_0}; 0)$.

σ_1 and its derivative sphere $\dot{\sigma}_1$. The whole Dupin cyclide is the curve defined by $\Lambda^4 \cap \mathcal{P}_1$ where $\mathcal{P}_1$ is the affine plane generated by the point σ_1 and the space-like vector $\overrightarrow{\dot{\sigma}_1}$ and the light-like vector $\overrightarrow{m_0}$. The control points of the rational quadratic Bézier curve in the Minkowski–Lorentz space which model the Dupin cyclide patch in $\mathcal{E}_3$ are given in the following Algorithm 2.

The centre Ω of the circle in $\mathcal{P}_1$ is the orthogonal projection of the centre O_5 of Λ^4 on the plane $\mathcal{P}_1$. After some computations, it yields:

Lemma 1. *Let σ_1 be a point on Λ^4, $\dot{\sigma}_1$ its derivative sphere and $\overrightarrow{m_0}$ a light-like vector.*

Let $\mathcal{P}_1$ be the plane defined by the point σ_1, the space-like vector $\overrightarrow{\dot{\sigma}_1}$ and the light-like vector $\overrightarrow{m_0}$.
Let Ω be the centre of the circle $\Lambda^4 \cap \mathcal{P}_1$.
Then, Ω is determined by

$$\overrightarrow{O_5\Omega} = \overrightarrow{O_5\sigma_1} - \frac{\overrightarrow{O_5\sigma_1} \cdot \overrightarrow{m_0}}{\overrightarrow{\dot{\sigma}_1} \cdot \overrightarrow{m_0}} \overrightarrow{\dot{\sigma}_1} + \frac{\overrightarrow{O_5\sigma_1} \cdot \overrightarrow{m_0}}{\left(\overrightarrow{\dot{\sigma}_1} \cdot \overrightarrow{m_0}\right)^2} \overrightarrow{m_0} \tag{31}$$

Sketch of proof. The point Ω is defined by

$$\overrightarrow{O_5\Omega} = \overrightarrow{O_5\sigma_1} + \alpha\,\overrightarrow{\dot{\sigma}_1} + \beta\,\overrightarrow{m_0}$$

where α and β are obtained by solving the following system

$$\begin{cases} \overrightarrow{O_5\Omega} \cdot \overrightarrow{\dot{\sigma}_1} = 0 \\ \overrightarrow{O_5\Omega} \cdot \overrightarrow{m_0} = 0 \end{cases} \quad \square \tag{32}$$

If the control points of the rational quadratic Bézier curve γ are three weighted points $(\sigma_0; \omega_0)$, $(P_1; \omega_1)$ and $(\sigma_2; \omega_2)$, and if Ω is the centre of the circle arc defined by γ, then the vectors $\overrightarrow{\Omega\sigma_0}$ (resp. $\overrightarrow{\Omega\sigma_2}$) and $\overrightarrow{\sigma_0 P_1}$ (resp. $\overrightarrow{\sigma_2 P_1}$) are orthogonal. This result is still true, due to

$$\begin{cases} \overrightarrow{\Omega\sigma_1} \cdot \overrightarrow{\sigma_1 P_1} = 0 \\ \overrightarrow{\Omega P_1} \cdot \overrightarrow{m_0} = 0 \end{cases}$$

Moreover, the vectors of $\overrightarrow{\mathcal{P}_1}$ orthogonal to $\overrightarrow{m_0}$ are the vectors parallel to $\overrightarrow{m_0}$. Then, the point P_1 belongs to the asymptote, defined by the point Ω and the vector $\overrightarrow{m_0}$ of this circle and,

$$\overrightarrow{\Omega P_1} = t_1\,\overrightarrow{m_0}$$

where t_1 is unknown. This value is obtained from the second orthogonal property

$$\overrightarrow{\Omega\sigma_1} \cdot \overrightarrow{\sigma_1 P_1} = 0$$

and that provides

$$t_1 = \frac{\overrightarrow{\Omega\sigma_1}^2}{\overrightarrow{m_0} \cdot \overrightarrow{\Omega\sigma_1}}$$

The last step consists in the computation of the weight ω_1. The control mass points of the rational quadratic Bézier curve are $(\sigma_1; 1)$, $(P_1; \omega_1)$ and $(\overrightarrow{m_0}; 0)$, and the expression of the aforementioned curve is

$$\begin{aligned}\overrightarrow{O_5\sigma(t)} &= \frac{1}{B_0(t) + \omega_1 B_1(t)} \left(B_0(t) \overrightarrow{O_5\sigma_1} + B_2(t) \overrightarrow{m_0} \right) \\ &+ \frac{\omega_1 B_1(t)}{B_0(t) + \omega_1 B_1(t)} \overrightarrow{O_5P_1}\end{aligned}$$

The weight ω_1 is computed by forcing $\sigma\left(\frac{1}{2}\right)$ to lie on Λ^4

$$\overrightarrow{O_5\sigma\left(\frac{1}{2}\right)} = \frac{1}{1+2\omega_1} \left(\overrightarrow{O_5\sigma_1} + 2\omega_1 \overrightarrow{O_5P_1} + \overrightarrow{m_0} \right)$$

which leads to

$$\begin{aligned}\sigma\left(\frac{1}{2}\right) \in \Lambda^4 &\iff \overrightarrow{O_5\sigma\left(\frac{1}{2}\right)} \cdot \overrightarrow{O_5\sigma\left(\frac{1}{2}\right)} = 1 \\ &\iff (1+2\omega_1)^2 = \left(\overrightarrow{O_5\sigma_1} + 2\omega_1 \overrightarrow{O_5P_1} + \overrightarrow{m_0} \right)^2\end{aligned}$$

which is equivalent to

$$(1+2\omega_1)^2 = \left((1+2\omega_1) \overrightarrow{O_5\sigma_1} + 2\omega_1 \overrightarrow{\sigma_1P_1} + \overrightarrow{m_0} \right)^2 \tag{33}$$

Recall that $\overrightarrow{O_5\sigma_1} \cdot \overrightarrow{\sigma_1P_1} = 0$, $\overrightarrow{O_5\sigma_1}^2 = 1$, $\overrightarrow{m_0}^2 = 0$ and

$$\overrightarrow{O_5\sigma_1} \cdot \overrightarrow{m_0} = \underbrace{\overrightarrow{O_5\Omega} \cdot \overrightarrow{m_0}}_{=0} + \overrightarrow{\Omega\sigma_1} \cdot \overrightarrow{m_0} = \overrightarrow{\Omega\sigma_1} \cdot \overrightarrow{m_0}$$

on one hand and

$$\overrightarrow{\sigma_1P_1} \cdot \overrightarrow{m_0} = \overrightarrow{\sigma_1\Omega} \cdot \overrightarrow{m_0} + \underbrace{\overrightarrow{\Omega P_1} \cdot \overrightarrow{m_0}}_{=0} = \overrightarrow{\sigma_1\Omega} \cdot \overrightarrow{m_0}$$

on the other hand. Formula (33) becomes

$$0 = 4\omega_1^2 \overrightarrow{\sigma_1P_1}^2 + 2(1+2\omega_1) \overrightarrow{O_5\sigma_1} \cdot \overrightarrow{m_0} + 4\omega_1 \overrightarrow{\sigma_1P_1} \cdot \overrightarrow{m_0} \tag{34}$$

which is equivalent to

$$4\omega_1^2 \overrightarrow{\sigma_1P_1}^2 = -2 \overrightarrow{O_5\sigma_1} \cdot \overrightarrow{m} \tag{35}$$

and then Formula (30) is obtained. Computing in space of spheres eases the calculations due to simplifications.

4.1.3. Canal surface defined by a characteristic circle and a sphere

This section deals with a characteristic circle C_1 and a sphere S_2. The circle is defined by two orthogonal spheres S_1 and $\dot{S}_1$. The representation on Λ^4 of these spheres are σ_2, σ_1 and $\dot{\sigma}_1$ respectively. On Λ^4, consider the circle passing through the points σ_1 and σ_2 such as the tangent vector to this circle at σ_1 is parallel to $\overrightarrow{\dot{\sigma}_1}$. The centre O_0 of this circle is defined by

$$\overrightarrow{\sigma_1O_0} = \alpha \overrightarrow{\sigma_1\sigma_2} + \beta \overrightarrow{\dot{\sigma}_1}$$

where α and β are unknown. These values are computed by solving the system

$$\begin{cases} \overrightarrow{\sigma_1O_0} \cdot \overrightarrow{\dot{\sigma}_1} = 0 \\ \overrightarrow{O_0I} \cdot \overrightarrow{\sigma_1\sigma_2} = 0 \end{cases} \tag{36}$$

where I is the midpoint of the segment $[\sigma_1\sigma_2]$. Two cases happen:

- The first one when $\overrightarrow{\sigma_2\sigma_1} \cdot \overrightarrow{O_5\dot{\sigma}_1} = 0$
  The segment $[\sigma_1\sigma_2]$ is a diameter of the circle. The intermediate control point is defined by

$$\overrightarrow{P_1} = \frac{\sqrt{\left|\overrightarrow{\sigma_0\sigma_2}^2\right|}}{2}\,\overrightarrow{\dot{\sigma}_1} \tag{37}$$

  The weight ω_2 verifies the relationship

$$\frac{1}{4}\overrightarrow{\sigma_1\sigma_2}^2 = \frac{\left|\overrightarrow{\sigma_0\sigma_2}^2\right|}{4}\,\omega_2\,\overrightarrow{\dot{\sigma}_1}^2$$

  Then, if $\overrightarrow{\sigma_1\sigma_2}^2$ is positive, the circle is connected and $\omega_2 = 1$, else the circle has two connected components and $\omega_2 = -1$. The semi-circle is defined by a rational quadratic Bézier curve with control mass points $(\sigma_1; 1)$, $\left(\overrightarrow{P_1}; 0\right)$ and $(\sigma_2; \omega_2)$.

- The second one when $\overrightarrow{\sigma_2\sigma_1} \cdot \overrightarrow{O_5\dot{\sigma}_1} \neq 0$
  The resolution of the system (36) leads to

$$\begin{aligned}\overrightarrow{\sigma_1 O_0} \;=\; & \frac{1}{2}\frac{\overrightarrow{\sigma_1\sigma_2}^2}{\overrightarrow{\sigma_1\sigma_2}^2 - \left(\overrightarrow{\sigma_2}\cdot\overrightarrow{\dot{\sigma}_1}\right)^2}\,\overrightarrow{\sigma_1\sigma_2} \\ & - \frac{1}{2}\frac{\overrightarrow{\sigma_1\sigma_2}^2 \times \left(\overrightarrow{\sigma_1\sigma_2}\cdot\overrightarrow{O_5\dot{\sigma}_1}\right)}{\overrightarrow{\sigma_1\sigma_2}^2 - \left(\overrightarrow{\sigma_2}\cdot\overrightarrow{\dot{\sigma}_1}\right)^2}\,\overrightarrow{O_5\dot{\sigma}_1}\end{aligned} \tag{38}$$

  To determine the point P_1 and the weight ω_1, it is enough to change the Euclidean product into the Lorentz product in Formulae given in Garnier (2007). Recall that I_1 is the midpoint of the segment $[\sigma_1\sigma_2]$. Then

$$\overrightarrow{I_1P_1} = t_1\overrightarrow{O_0I_1} \quad \text{with} \quad t_1 = \frac{\overrightarrow{O_0\sigma_1}\cdot\overrightarrow{I_1\sigma_1}}{\overrightarrow{O_0\sigma_0}\cdot\overrightarrow{O_0I_1}} \tag{39}$$

  and

$$\omega_1 = \frac{\left|\overrightarrow{\sigma_0P_1}\cdot\overrightarrow{\sigma_0\sigma_2}\right|}{\sqrt{\overrightarrow{\sigma_0P_1}^2 \times \overrightarrow{\sigma_0\sigma_2}^2}} \tag{40}$$

  the circle arc is modelled by a rational quadratic Bézier curve with control mass points $(\sigma_0; 1)$, $(P_1; \omega_1)$ and $(\sigma_2; 1)$. To obtain the other arc of this circle, $(P_1; \omega_1)$ is replaced by $(P_1; -\omega_1)$.

Now, an example on how to construct a seahorse using rational quadratic Bézier curves in the Minkowski–Lorentz space is given: in $\mathcal{E}_3$, the surfaces are Dupin cyclide patches. Each curve in this space models a canal surface in $\mathcal{E}_3$. The G^1 blends between two canal surfaces is carried out by the G^1 blends between these Bézier curves.

The G^1 blends of curves is simplest using Bézier curves. The middle control points P_1 defines the tangent to the curve at σ_0 and σ_2. The derivative sphere $\dot{\sigma}_0$ of σ_0 is defined by

$$\overrightarrow{O_5\dot{\sigma}_0} = \overrightarrow{\dot{\sigma}_0} = \frac{1}{\sqrt{\overrightarrow{P_1\sigma_0}^2}}\,\overrightarrow{\sigma_0P_1} \tag{41}$$

whereas the derivative sphere $\dot{\sigma}_2$ of σ_2 is defined by

$$\overrightarrow{O_5\dot{\sigma}_2} = \overrightarrow{\dot{\sigma}_2} = \frac{1}{\sqrt{\overrightarrow{P_1\sigma_2}^2}}\,\overrightarrow{P_1\sigma_2} \tag{42}$$

In fact, in formulae (41) and (42), the direction vectors is irrelevant: the orientations of the derivative spheres would be opposite but the characteristic circle is the same.

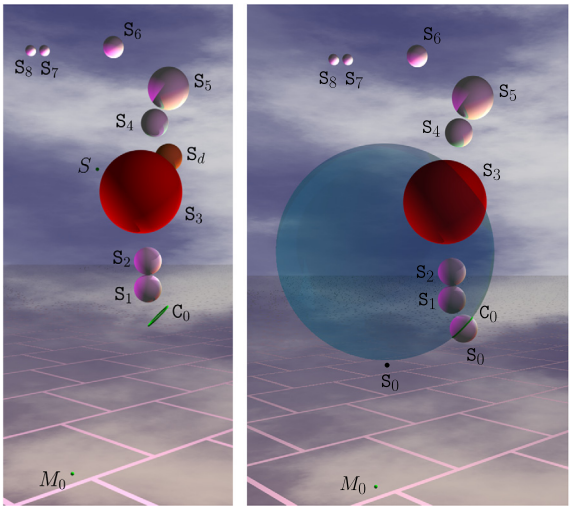

(a) (b)

Fig. 6. Constraints which define a seahorse. (a): Spheres, a circle and a point. (b): Choice of the sphere $\mathbb{S}_0$ and its derivative sphere $\dot{\mathbb{S}}_0$.

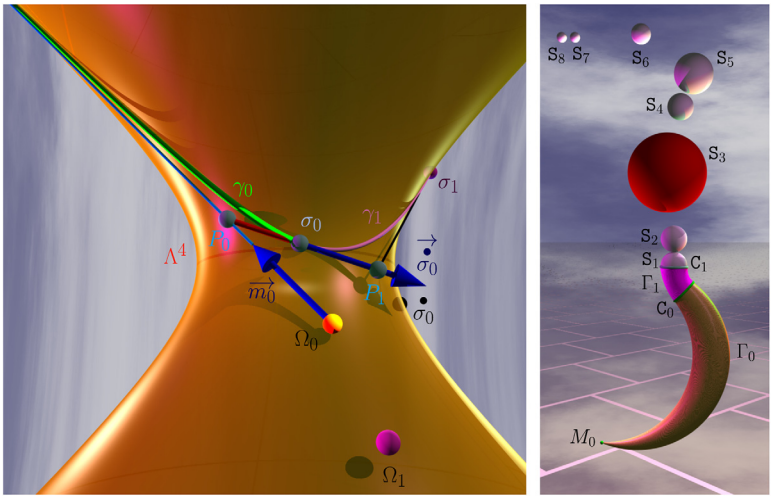

(a) (b)

Fig. 7. The first and second steps of the construction of the seahorse. (a): On Λ^4, G^1 blend of two Bézier curves which define a G^1 blend of two canal surfaces composing the seahorse. (b): G^1 blend of the canal surfaces Γ_0 and Γ_1 obtained in $\mathcal{E}_3$.

4.2. G^1 connections

The constraints which design the tail, the body and the head are the spheres $\mathbb{S}_i$, i belongs to $[\![1;8]\!]$, see Fig. 6(a) and Table 2 in Garnier et al. (2016).

The seahorse tail is obtained by a point M_0 and a circle $\mathbb{C}_0$, see Fig. 6(a) e.g. two orthogonal spheres of the pencil of spheres of base C, see Fig. 6(b).

In the Minkowski–Lorentz space, the representation of the tail is done by the intersection of Λ^4 and the 2-plane defined by the point σ_0, the light-like vector $\vec{m_0}$ and the space-like vector $\vec{\sigma_0}$ which define the Bézier curve γ_0, see Algorithm 2. The determination of the BR curve γ_1 defined by σ_0, $\dot{\sigma}_0$ and σ_1 is done using section 4.1.3. Fig. 7(a) shows the first two steps: the light-like vector $\vec{m_0}$ which represents the point M_0; the points σ_0 and $\dot{\sigma}_0$ on Λ^4 which represent the sphere $\mathbb{S}_0$ and its derivative sphere $\dot{\mathbb{S}}_0$; the space-like tangent vector $\vec{\dot{\sigma}_0}$ to the Bézier curve γ_0 at the point σ_0; the centre Ω_0 of the first circle; the control point P_0 of the curve γ_0; the asymptote of the circle defined by the point Ω and the light-like vector $\vec{m_0}$; the sphere σ_1 on Λ^4 which is the second endpoint of the curve γ_1; the control point P_1 of the curve γ_1; the two Bézier curves γ_0 and γ_1.

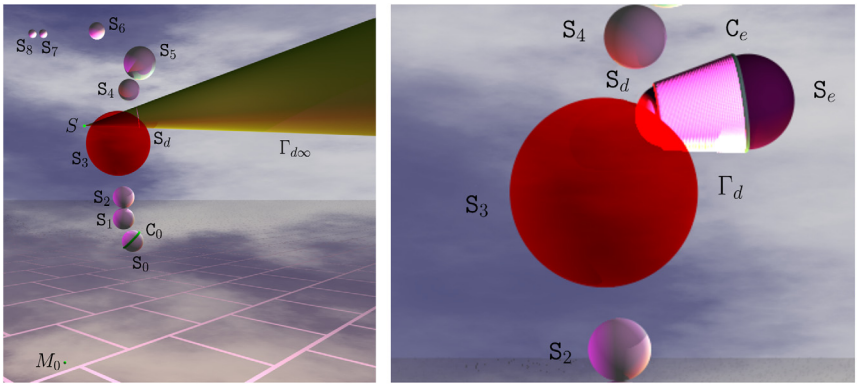

(a) (b)

Fig. 8. The dorsal fin of the seahorse. (a): The circular cone $\Gamma_{d\infty}$ containing the dorsal fin of the seahorse. (b): The useful part of the previous circular cone.

The joint between γ_0 and γ_1 at the point σ_0 is G^1 and the tangent vectors to the curves γ_0 and γ_1 at σ_0 are parallel to the vector $\overrightarrow{\dot{\sigma}_0}$.

Fig. 7(b) shows the G^1 blend of the two canal surfaces defined by the Bézier curves in the Minkowski–Lorentz space. The other canal surfaces for the body and for the head are computed in the same way.

Now, the dorsal fin is computed. From the point $S\left(\frac{-25}{3}, 0, \frac{43}{3}\right)$ and the sphere $\mathbb{S}_d$ of centre $O_d\,(2, 0, 16)$ of radius $r_d = 2$, the output of Algorithm 1 is a circular cone defined by the Bézier curve $\gamma_{d\infty}$ of control mass points $\left(\overrightarrow{s}; 0\right)$, $(\Omega_d; \omega_d)$ and $\left(\overrightarrow{e_\infty}; 0\right)$, Fig. 8(a). A point $\sigma\,(t)$, $t \in [0; 1]$, belongs to the curve $\gamma_{d\infty}$ iff

$$\overrightarrow{O_5\sigma\,(t)} = \frac{1}{\omega_d B_1\,(t)}\left(B_0\,(t)\,\overrightarrow{s} + \omega_d B_1\,(t)\,\overrightarrow{O_5\Omega_d} + B_2\,(t)\,\overrightarrow{e_\infty}\right)$$

and the radius of the sphere defined by $\sigma\,(t)$ is computed using the first component (e.g. the component of $\overrightarrow{e_o}$), and

$$\frac{1}{\rho\,(t)} = \frac{1}{\omega_d B_1\,(t)}\left(B_0\,(t) - \frac{\omega_d B_1\,(t)}{\rho_d}\underbrace{\overrightarrow{O_5\Omega_d}\cdot\overrightarrow{e_\infty}}_{=0}\right) = \frac{B_0\,(t)}{\omega_d B_1\,(t)} \tag{43}$$

and the solution of this equation is resulting from Lemma 2.

Lemma 2. *: The solution of equation (43) is*

$$t_0 = \frac{\rho_0}{2\,\omega_d + \rho_0} \tag{44}$$

Proof. Equation (43) can be simplified into

$$\frac{1}{\rho_0} = \frac{1 - t_0}{2\,\omega_d\,t_0}$$

which leads to equation (44). □

The useful part of the circular cone is computed. One of the bound of this cone is the sphere $\mathbb{S}_d$ of radius $r_d = 2$. The choice of the second is the sphere $\mathbb{S}_e$ of radius $r_e = 3$. From the radii r_d and r_e, the parameters t_d and t_e of the Bézier curve are computed using Lemma 2 and the solutions are $t_d \simeq 0879$ and $t_e \simeq 0.916$. The expression of the homography, Theorem 1 in Garnier and Bécar (2016), is

$$h\,(u) = \frac{\dfrac{t_d}{\sqrt{\omega_d\,B_1\,(t_d)}}\,(1-u) + \dfrac{t_e}{\sqrt{\omega_d\,B_1\,(t_e)}}\,u}{\dfrac{1}{\sqrt{\omega_d\,B_1\,(t_d)}}\,(1-u) + \dfrac{1}{\sqrt{\omega_d\,B_1\,(t_e)}}\,u}$$

and the endpoints of the new Bézier curve are $(\sigma_d; 1)$ and $(\sigma_e; 1)$. The intermediate control mass point is

$$(P_e, \omega_e) \simeq ((0.4000, 1.8333, 0, 6.5667, 55.5333)\,, 1.021)$$

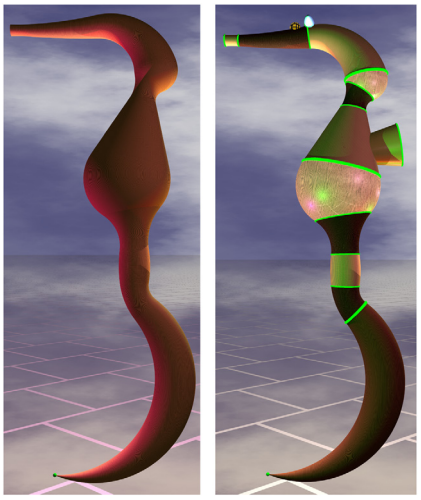

(a) (b)

Fig. 9. A seahorse modelled by G^1 blends of canal surfaces, each surface is represented by a rational quadratic Bézier curve in the Minkowski–Lorentz space. The joints between two Bézier curves are G^1. (a): The seahorse without the dorsal fin. (b): The whole seahorse.

Fig. 10. A zoom of a seahorse part to show G^1 blends of canal surfaces.

To complete the construction of the seahorse, two eyes are added. They are modelled by two spheres of radius $\frac{r_6}{2}$, the centres $\mathscr{T}_{\overrightarrow{u}}(O_6)$ and $\mathscr{T}_{\overrightarrow{v}}(O_6)$ where: $\mathscr{T}_{\overrightarrow{w}}$ designate the translation of vector $\overrightarrow{w}$; the components of $\overrightarrow{u}$ are $\left(-2, \frac{3}{2}, 1\right)$; the components of $\overrightarrow{v}$ are $\left(-2, -\frac{3}{2}, 1\right)$.

The coronet of the seahorse is modelled by an ellipsoid of semi-axes $\frac{r_6}{2}$, $\frac{9\,r_6}{4}$ and $\frac{r_6}{2}$. The centre of this ellipsoid is $\mathscr{T}_{r_6\overrightarrow{k}}(O_6)$.

Fig. 9(a) shows the seahorse without the dorsal fin, the material is the same to show the G^1 blends. Fig. 10 shows a zoom of the seahorse to illustrate the G^1 blends between some canal surfaces. Fig. 9(b) shows the whole seahorse.

5. Conclusion

The paper deals with the use of mass points in order to design conics as quadratic Bézier curves. These curves are embedded in the Minkowski–Lorentz space. Some elements in that space are presented and used for computer aided design purposes as the space of oriented spheres, the canal surfaces and Dupin cyclides. The authors propose the algorithms that ease, in the Minkowski–Lorentz space, the computation of Dupin cyclides patches and their G^1 connection. A schematic seahorse built and based from all previous results ends the paper.

Working with the space of spheres provides a new and easy proof of the famous Dandelin theorem on spheres in a cone. This work is carried out on the iterative construction of the characteristic circles of Dupin cyclides based on the subdivision algorithms of Bézier curves. The G^1 connections in this article shown with a seahorse sketch lead the authors to the idea that the G^2 connection could be completed with that process after new investigation. An other way is the use of the Minkowski–Lorentz space and the space of spheres to pair points on a boundary of a planar skeleton of a canal surface.

Acknowledgements

The authors warmly thank Professor Ron Goldman from Rice University in Houston for his review and his helpful comments.

Appendix A. Recalls of Minkowski–Lorentz space and space of spheres

A.1. Equivalent representations of elements in $\mathcal{E}_3$ and Minkowski–Lorentz space

Type	$\mathcal{E}_3 \cup \{\infty\}$	$L_{4,1}$ or $\overrightarrow{L_{4,1}}$	Property
Point	$P \in \mathcal{E}_3$	$\overrightarrow{p} = \overrightarrow{e_o} + \overrightarrow{O_3P} + \frac{\left\|\overrightarrow{O_3P}\right\|^2}{2}\overrightarrow{e_\infty}$	$\overrightarrow{p}^2 = 0$
	∞	$\overrightarrow{e_\infty}$	$\overrightarrow{e_\infty}^2 = 0$
Sphere	Centre Ω	$\overrightarrow{O_5\sigma} = \frac{1}{\rho}\left(\overrightarrow{e_o} + \overrightarrow{\Omega} + \frac{1}{2}\left(\left\|\overrightarrow{\Omega}\right\|^2 - \rho^2\right)\overrightarrow{e_\infty}\right)$	$\overrightarrow{O_5\sigma}^2 = 1$
	Radius ρ		
Plane $\mathcal{P}$	Normal vector $\overrightarrow{N}$	$\overrightarrow{O_5\pi} = \overrightarrow{N} + \left(\overrightarrow{N} \bullet \overrightarrow{P}\right)\overrightarrow{e_\infty}$	$\overrightarrow{O_5\pi}^2 = 1$
	Point $P \in \mathcal{P}$		

A.2. Properties of points and spheres

Type	$\mathcal{E}_3 \cup \{\infty\}$	$L_{4,1}$ or $\overrightarrow{L_{4,1}}$	Property
Point	P	$\overrightarrow{p}$	$P \in S \Longleftrightarrow \overrightarrow{p} \,.\, \overrightarrow{O_5\sigma} = 0$
Sphere	S	$\sigma \in \Lambda^4$	$P \in \mathcal{P} \Longleftrightarrow \overrightarrow{p} \,.\, \overrightarrow{O_5\pi} = 0$
Plane	$\mathcal{P}$	$\pi \in \Lambda^4$	$\overrightarrow{e_\infty} \,.\, \overrightarrow{O_5\pi} = 0$
Sphere	S_1	σ_1	$S_1 \perp S_2 \Longleftrightarrow \overrightarrow{O_5\sigma_1} \,.\, \overrightarrow{O_5\sigma_2} = 0$
			$\#(S_1 \cap S_2) > \{1\} \Longleftrightarrow \left\|\overrightarrow{O_5\sigma_1} \,.\, \overrightarrow{O_5\sigma_2}\right\| < 1$
Sphere	S_2	σ_2	S_1 and S_2 are tangent $\Longleftrightarrow \left\|\overrightarrow{O_5\sigma_1} \,.\, \overrightarrow{O_5\sigma_2}\right\| = 1$
			$S_1 \cap S_2 = \emptyset \Longleftrightarrow \left\|\overrightarrow{O_5\sigma_1} \,.\, \overrightarrow{O_5\sigma_2}\right\| > 1$

If the orientation of the tangent spheres S_1 and S_2 at P is the same, then

$$\overrightarrow{O_5\sigma_1} \,.\, \overrightarrow{O_5\sigma_2} = 1$$

and

$$\overrightarrow{\sigma_1\sigma_2}^2 = 0$$

and the vectors $\overrightarrow{\sigma_1\sigma_2}$ and $\overrightarrow{p}$ are parallel. Moreover, the direction of the vector $\overrightarrow{\sigma_1\sigma_2}$ in $\overrightarrow{L_{4,1}}$ defines, in $\mathcal{E}_3$, the point of tangency between the spheres S_1 and S_2.

A.3. Dupin cyclides as rational quadratic Bézier curves

A.3.1. A branch of a circle which model a circular cone, a horned Dupin cyclide or a spindle Dupin cyclide

Constraints in $\mathcal{E}_3$ and representation in the Minkowski–Lorentz space: two points[3] $M_0 \rightleftarrows \overrightarrow{m_0}$ and $M_2 \rightleftarrows \overrightarrow{m_2}$ of $\mathcal{E}_3 \cup \{\infty\}$ and a non-degenerate sphere[4] $S \rightleftarrows \sigma$, Fig. A.11.

[3] The representation of the point M_0 in $\mathcal{E}_3$ is the light-like vector $\overrightarrow{m_0}$ in $\overrightarrow{L_{4,1}}$.

[4] The representation of the plane or the sphere S in $\mathcal{E}_3$ is the point σ on the unit (4-dimensional-)sphere Λ^4 in $L_{4,1}$.

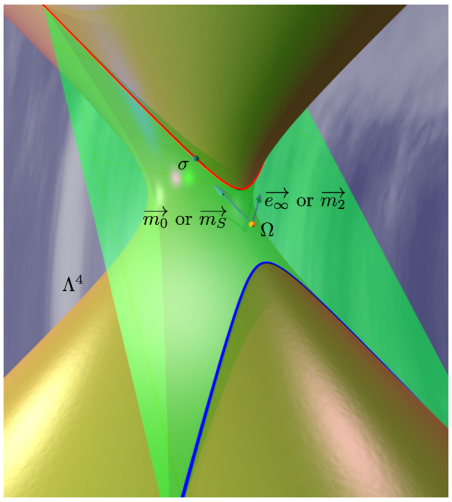

Fig. A.11. A semi-circular cone, a horned or spindle Dupin cyclide part bounded by the singular points modelled by a Bézier curve with control mass points.

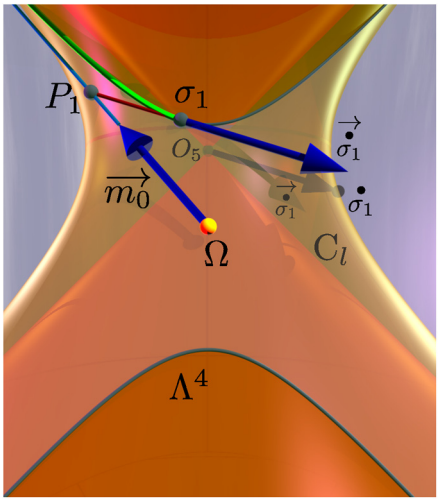

Fig. A.12. A circular cone part, a horned or spindle Dupin cyclide part bounded by a circle (intersection of two orthogonal spheres) and a point modelled by a Bézier curve with control mass points.

The centre of the circle is Ω, orthogonal projection of O_5 onto the plane defined by σ, $\overrightarrow{m_0}$ and $\overrightarrow{m_2}$.

Control mass points of the Bézier curve: $(\overrightarrow{m_0}; 0)$, $\left(\Omega; \pm\sqrt{\frac{1}{2}\frac{\overrightarrow{m_0}\cdot\overrightarrow{m_2}}{1-\overrightarrow{O_5\Omega}^2}}\right)$ and $(\overrightarrow{m_2}; 0)$ and it is possible to use $\overrightarrow{e_\infty}$ instead of $\overrightarrow{m_2}$, and the vertex of the cone is $M_0 = M_S$, see Algorithm 1.

A.3.2. An arc of a branch of a circle

Constraints in $\mathcal{E}_3$: a point $M_0 \rightleftarrows \overrightarrow{m_0}$ and two orthogonal spheres $S_1 \rightleftarrows \sigma_1$ and $\dot{S}_1 \rightleftarrows \dot{\sigma}_1$.

The centre of the circle is Ω, orthogonal projection of O_5 onto the plane defined by σ_1, $\overrightarrow{m_0}$ and $\overrightarrow{O_5\dot{\sigma}_1}$.
The intermediate control point P_1 is defined by:

$$\overrightarrow{\Omega P_1} = \frac{\overrightarrow{\Omega\sigma_1}^2}{\overrightarrow{m_0}\cdot\overrightarrow{\Omega\sigma_1}}\overrightarrow{m_0}$$

Control mass points of the Bézier curve: $(\sigma_1; 1)$, $\left(P_1; \pm\sqrt{-\frac{\overrightarrow{O_5\sigma_1}\cdot\overrightarrow{m_0}}{2\,\overrightarrow{\sigma_1 P_1}^2}}\right)$ and $(\overrightarrow{m_0}; 0)$, Algorithm 2, and it is possible to use $\overrightarrow{e_\infty}$ instead of $\overrightarrow{m_0}$, Fig. A.12.

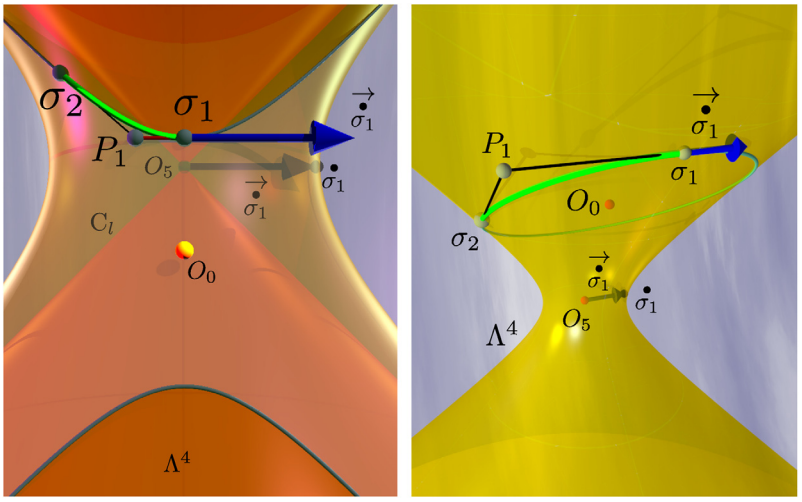

Fig. A.13. A Dupin cyclide part without singular points modelled by a Bézier curve with control mass points. (a): A circular cone, a horned or spindle Dupin cyclide. (b): A ring Dupin cyclide.

A.3.3. An arc of a circle

Constraints in $\mathcal{E}_3$: two orthogonal spheres $\mathbb{S}_1 \rightleftarrows \sigma_1$ and $\dot{S}_1 \rightleftarrows \dot{\sigma_1}$ and a non-degenerate sphere $\mathbb{S}_2 \rightleftarrows \sigma_2$.

The centre of the circle is O_0, orthogonal projection of O_5 onto the plane defined by σ_1, $\overrightarrow{m_0}$ and $\overrightarrow{O_5\dot{\sigma_1}}$. O_5 is not the midpoint I of the segment $[\sigma_1\sigma_2]$.

The intermediate control point P_1 is defined by

$$\overrightarrow{I_1P_1} = \frac{\overrightarrow{O_0\sigma_1} \cdot \overrightarrow{I_1\sigma_1}}{\overrightarrow{O_0\sigma_0} \cdot \overrightarrow{O_0I_1}} \quad \overrightarrow{O_0I_1}$$

Control mass points of the Bézier curve: $(\sigma_1; 1)$, $\left(P_1; \frac{\left|\overrightarrow{\sigma_0P_1} \cdot \overrightarrow{\sigma_0\sigma_2}\right|}{\sqrt{\overrightarrow{\sigma_0P_1}^2 \times \overrightarrow{\sigma_0\sigma_2}^2}}\right)$ and $(\sigma_2; 1)$, section 4.1.3, Fig. A.13.

The reader can see an animation on a Dupin cyclide becoming a cone following the link: http://ufrsciencestech.u-bourgogne.fr/~garnier/publications/refigCD4EN2Cone26.gif.

References

Albrecht, Gudrun, 2001. Determination of geometrical invariants of rationally parametrized conic sections. In: Mathematical Methods for Curves and Surfaces. Vanderbilt University, Nashville, TN, USA, pp. 15–24.

Albrecht, G., Bécar, J.-P., Farin, Gerald E., Hansford, Dianne, 2008. On the approximation order of tangent estimators. Comput. Aided Geom. Des. 25 (2), 80–95.

Bécar, J.P., 1997. Forme (BR) des coniques et de leurs faisceaux. PhD thesis. Université de Valenciennes et de Hainaut-Cambrésis, LIMAV.

Bécar, J.P., Druoton, L., Fuchs, L., Garnier, L., Langevin, R., Morin, G., 2016. Espace de Minkowski–Lorentz et espace des sphères: un état de l'art. In: GTMG 2016. Dijon, France. Le2i, Université de Bourgogne.

Bézier, P., 1986. Courbe et surface, vol. 4, 2ème edition. Hermès, Paris.

De Casteljau, P., 1985. Mathématiques et CAO. Volume 2: formes à pôles. Hermes.

Dorst, Leo, Fontijne, Daniel, Mann, Stephen, 2007. Geometric Algebra for Computer Science: An Object Oriented Approach to Geometry. Morgan Kauffmann Publishers.

Druoton, L., 2013. Recollements de morceaux de cyclides de Dupin pour la modélisation et la reconstruction 3D. PhD thesis. Université de Bourgogne, Institut de Mathématiques de Bourgogne.

Druoton, L., Fuchs, L., Garnier, L., Langevin, R., 2014. The non-degenerate Dupin cyclides in the space of spheres using geometric algebra. Adv. Appl. Clifford Algebras (ISSN 0188-7009) 23 (4), 787–990.

Druoton, L., Garnier, L., Langevin, R., 2013a. Iterative construction of Dupin cyclide characteristic circles using non-stationary Iterated Function Systems (IFS). Comput. Aided Des. 45 (2), 568–573. Solid and Physical Modeling 2012, Dijon.

Druoton, L., Langevin, R., Garnier, L., 2013b. Blending canal surfaces along given circles using Dupin cyclides. Int. J. Comput. Math., 1–20.

Dutta, D., Martin, R.R., Pratt, M.J., 1993. Cyclides in surface and solid modeling. IEEE Comput. Graph. Appl. 13 (1), 53–59.

Farin, Gerald, 1992. From conics to NURBS: a tutorial and survey. IEEE Comput. Graph. Appl. 12 (5), 78–86.

Fiorot, J.C., Jeannin, P., 1989. Courbes et surfaces rationnelles. RMA, vol. 12. Masson.

Foufou, S., Garnier, L., 2004. Dupin cyclides as quadrics blends for shape modeling. In: Eurographic's 2004, vol. 23, pp. 321–330.

Garnier, L., 2007. Mathématiques pour la modélisation géométrique, la représentation 3D et la synthèse d'images. Ellipses. ISBN 978-2-7298-3412-8.

Garnier, Lionel, Bécar, Jean-Paul, 2016. Mass points, Bézier curves and conics: a survey. In: Eleventh International Workshop on Automated Deduction in Geometry, Proceedings of ADG 2016. Strasbourg, France, pp. 97–116. http://ufrsciencestech.u-bourgogne.fr/~garnier/publications/adg2016/.

Garnier, L., Bécar, J.P., 2017. Nouveaux modèles géométriques pour la C.A.O. et la synthèse d'images : courbes de Bézier, points massiques et surfaces canal. Editions Universitaires Européennes, Saarbrucken. ISBN 978-3-639-54676-7.
Garnier, L., Bécar, J.P., Druoton, L., 2016. Surfaces canal et courbes de Bézier rationnelles quadratiques. Université de Bourgogne, Le2i, Dijon, France. http://ufrsciencestech.u-bourgogne.fr/~garnier/publications/hippocampe/.
Garnier, L., Druoton, L., 2013a. Constructions, dans l'espace des sphères, de carreaux de cyclides de Dupin à bords circulaires. Rev. Electron. Francoph. Inform. Gr. 7 (1), 17–40.
Garnier, L., Druoton, L., 2013b. Constructions of principal patches of Dupin cyclides defined by constraints: four vertices on a given circle and two perpendicular tangents at a vertex. In: XIV Mathematics of Surfaces. 11–13 September. Royaume-Uni, Birmingham, pp. 237–276.
Garnier, L., Druoton, L., 2013c. Inversions de coniques à centres vues comme des cercles. Université de Limoges, AFIG.
Garnier, L., Druoton, L., Bécar, J.P., 2015. Points massiques, espace des sphères et "hyperbole". In: G.T.M.G. 2015. Poitiers. http://gtmg2015.conference.univ-poitiers.fr/programme_details.
Garnier, L., Druoton, L., Langevin, R., 2012. Subdivisions itératives d'arcs d'ellipses et d'hyperboles et application à la visualisation de cyclides de Dupin. Rev. Electron. Francoph. Inform. Gr. 6 (2), 1–36.
Goldman, R.N., Wang, W., 2004. Using invariants to extract geometric characteristics of conic sections from rational quadratic parameterizations. Int. J. Comput. Geom. Appl. 14 (3), 161–187.
Langevin, R., Solanes, G., 2011. The geometry of canal surfaces and the length of curves in de sitter space. Adv. Geom. 11 (4), 585–601.
Langevin, R., Walczak, P.G., 2008. Conformal geometry of foliations. Geom. Dedic. 132 (5), 135–178.
Langevin, Rémi, Sifre, Jean-Claude, Druoton, Lucie, Garnier, Lionel, Paluszny, Marco, 2014. Finding a cyclide given three contact conditions. Comput. Appl. Math., 1–18.
Lee, E.T.Y., 1985. The rational Bézier representation for conics. In: Farin, G. (Ed.), Geometric Modeling, Algorithms and New Trends. SIAM, Philadelphia, pp. 3–19.
Piegl, L.A., Tiller, W., 1995. The NURBS Book. Monographs in Visual Communication. Springer.
Sánchez-Reyes, J., 2011. Characteristics of conic segments in Bézier form. In: International Conference on Innovative Methods in Product Design. Venise, Italy, pp. 231–234.
Versprille, Kenneth James, 1975. Computer-aided Design Applications of the Rational B-spline Approximation Form. PhD thesis. Syracuse, NY, USA. AAI7607690.